Current Biology 20, 2058–2065, November 23, 2010 ©2010 Elsevier Ltd All rights reserved DOI 10.1016/j.cub.2010.10.029

Report

TAp73 Acts via the bHLH Hey2 to Promote Long-Term Maintenance of Neural Precursors

Masashi Fujitani,[1,2] Gonzalo I. Cancino,[1,2,8] Chandrasagar B. Dugani,[1,2,3,8] Ian C.G. Weaver,[1,2] Andrée Gauthier-Fisher,[1,2] Annie Paquin,[1,2,3] Tak W. Mak,[4,7] Martin J. Wojtowicz,[5] Freda D. Miller,[2,3,5,6,*] and David R. Kaplan[1,3,6,*]

[1]Cell Biology
[2]Developmental and Stem Cell Biology Programs
Hospital for Sick Children, Toronto, Ontario M5G 1L7, Canada
[3]Institute for Medical Sciences
[4]Department of Medical Biophysics
[5]Department of Physiology
[6]Department of Molecular Genetics
University of Toronto, Toronto, Ontario M5S 1A8, Canada
[7]Cambell Family Institute for Breast Cancer Research, Ontario Cancer Institute, Toronto, Ontario M5G 2M9, Canada

Summary

Increasing evidence suggests that deficits in adult stem cell maintenance cause aberrant tissue repair and premature aging [1]. While the mechanisms regulating stem cell longevity are largely unknown, recent studies have implicated p53 and its family member p63. Both proteins regulate organismal aging [2–4] as well as survival and self-renewal of tissue stem cells [5–9]. Intriguingly, haploinsufficiency for a third family member, p73, causes age-related neurodegeneration [10]. While this phenotype is at least partially due to loss of the ΔNp73 isoform, a potent neuronal prosurvival protein [11–16], a recent study showed that mice lacking the other p73 isoform, TAp73, have perturbations in the hippocampal dentate gyrus [17], a major neurogenic site in the adult brain. These findings, and the link between the p53 family, stem cells, and aging, suggest that TAp73 might play a previously unanticipated role in maintenance of neural stem cells. Here, we have tested this hypothesis and show that TAp73 ensures normal adult neurogenesis by promoting the long-term maintenance of neural stem cells. Moreover, we show that TAp73 does this by transcriptionally regulating the bHLH Hey2, which itself promotes neural precursor maintenance by preventing premature differentiation.

Results

TAp73 Is Necessary to Promote Maintenance of Postnatal Dentate Gyrus Precursors

TAp73$^{-/-}$ [17] mice display an aberrant hippocampal dentate gyrus (DG), a phenotype of unknown etiology. To understand this, we characterized TAp73 expression and developmental onset of the phenotype. RT-PCR (Figure 1A) and immunostaining (Figure 1B) demonstrated that TAp73 is expressed in the newborn mouse hippocampus, where it is predominantly localized to nuclei of cells that coexpress Tbr2, a marker for type 2a precursors [18] (Figure 1B). To determine when the DG first became aberrant, we Nissl stained the postnatal hippocampus (Figure 1C and Figure S1A, available online); *TAp73*$^{-/-}$ and *TAp73*$^{+/+}$ hippocampi were morphologically similar at birth, started to show some differences at postnatal day 6 (P6), and by P16 the dorsal lower blade of the *TAp73*$^{-/-}$ DG was missing. Confirmation that the DG was similar at earlier time points was obtained by immunostaining newborn sections for nestin and prox1, markers for precursors and DG neurons, respectively (Figure S1B).

Because the region that becomes aberrant postnatally is comprised of the last-born DG neurons [19], this suggests that TAp73 is necessary for postnatal neurogenesis. To test this idea, we studied ongoing neurogenesis in the adult hippocampus [20]. Adult *TAp73*$^{-/-}$ and *TAp73*$^{+/+}$ mice were injected with BrdU, and hippocampi were analyzed immunocytochemically 24 hr later (Figure 1D). Quantification showed an almost 2-fold decrease in proliferating, BrdU-positive precursors in the *TAp73*$^{-/-}$ subgranular zone (SGZ; the location of the DG precursors) of both the lower and upper DG blades (Figures 1D and 1E). Similarly, doublecortin-positive newly born neurons (Figure 1D) were also reduced approximately 2-fold in the *TAp73*$^{-/-}$ DG (Figure 1F). Thus, TAp73 loss depletes adult DG precursors and decreases neurogenesis.

To ask whether this phenotype reflected a cell-intrinsic precursor deficit, we cultured *TAp73*$^{+/+}$ and *TAp73*$^{-/-}$ P3 hippocampal cells in FGF2 and EGF to generate neurospheres [21]. RT-PCR demonstrated that *TAp73*, *ΔNp73*, and *p53* mRNAs were expressed in DG neurospheres and that *ΔNp73* and *p53* mRNA levels were unaltered by loss of TAp73 (Figure 1G). Immunostaining confirmed that the majority of *TAp73*$^{+/+}$ but not *TAp73*$^{-/-}$ neurosphere cells expressed nuclear TAp73 (Figure 1H). Quantitative analysis at clonal density demonstrated that *TAp73*$^{+/+}$ and *TAp73*$^{-/-}$ neonatal hippocampi contained similar numbers of neurosphere-generating precursors (Figure 1I), consistent with the lack of an in vivo phenotype at birth. However, when sequentially passaged, the *TAp73*$^{-/-}$ neurosphere-forming cells were progressively depleted (Figure 1J), indicating that TAp73 is required for long-term precursor maintenance. In contrast, mean neurosphere diameter (Figure 1K) and Ki67-positive proliferating cells (Figures 1L and 1M) were unchanged, suggesting that TAp73 is not necessary for proliferation of biased progenitors, which comprise the majority of cells in the spheres.

Loss of TAp73 Depletes Adult SVZ Precursors and Decreases Olfactory Neurogenesis

To ask whether TAp73 is required for maintenance of other adult neural precursors, we examined olfactory neurogenesis, which is ongoing for the life of the animal [20]. Adult *TAp73*$^{+/+}$ and *TAp73*$^{-/-}$ mice were injected five times with BrdU over a 12 hr period. Quantitative immunocytochemical analysis of their olfactory bulbs 30 days later demonstrated an almost 2-fold decrease in BrdU-positive newly born neurons expressing the neuron-specific protein NeuN (Figures 2A and 2B and Figure S2A) in *TAp73*$^{-/-}$ mice. To ask whether this was due to depletion of precursors, we generated clonal neurospheres

*Correspondence: fredam@sickkids.ca (F.D.M.), dkaplan@sickkids.ca (D.R.K.)
[8]These authors contributed equally to this work

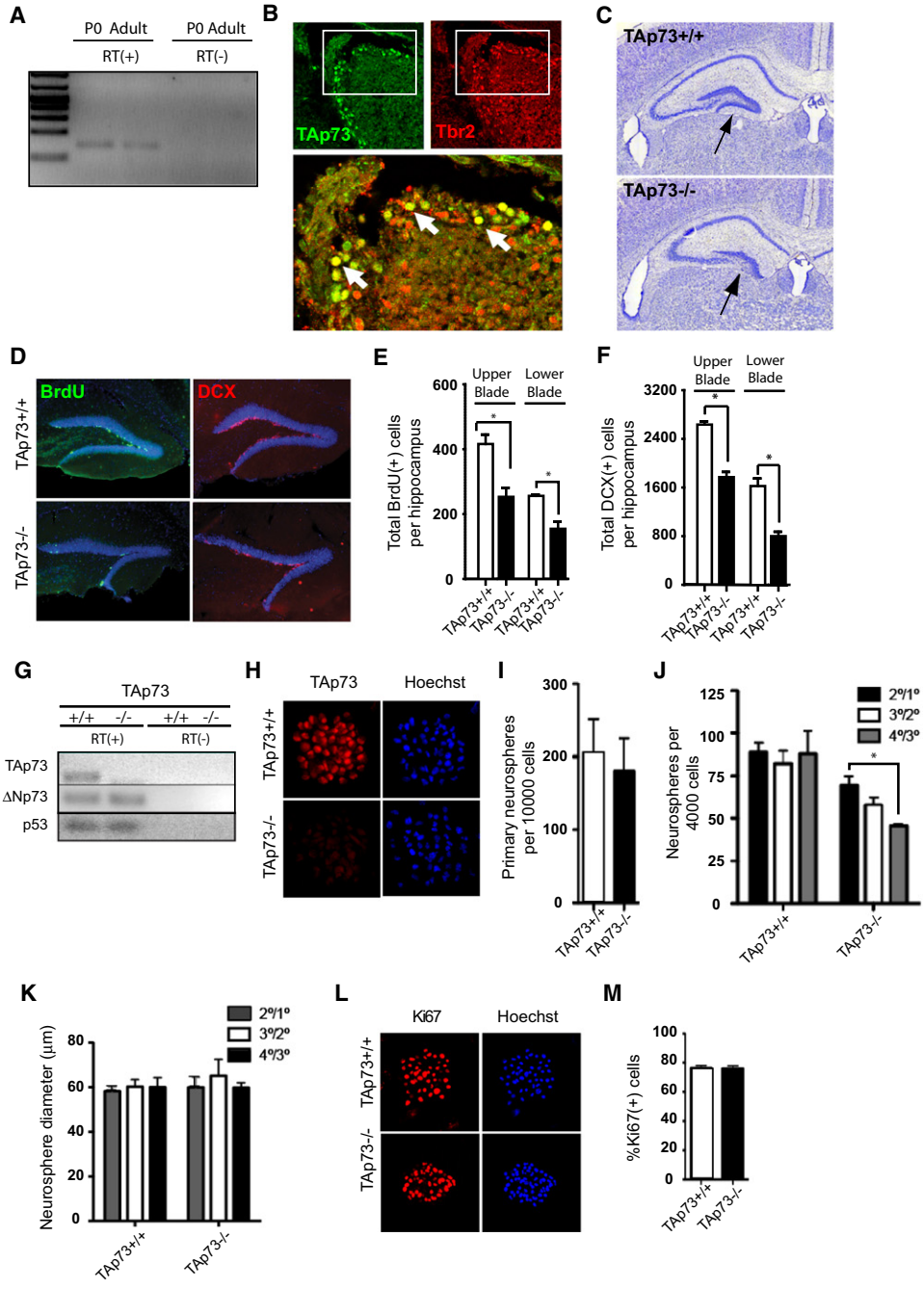

Figure 1. TAp73 Regulates Hippocampal DG Precursors and Neurogenesis

(A) RT-PCR analysis for *TAp73* mRNA in the postnatal (P0) and adult hippocampus. Negative controls lacked reverse transcriptase (RT−).

(B) Immunostaining for TAp73 (green) and Tbr2 (red) in a coronal section through the newborn DG. The boxed areas in the top panels are shown at higher magnification in the bottom panel. Arrows denote double-labeled cells.

(C) Nissl stained *TAp73*$^{+/+}$ versus *TAp73*$^{-/-}$ hippocampus at P16. Arrows indicate lower DG blade.

(D) DG of adult *TAp73*$^{+/+}$ versus *TAp73*$^{-/-}$ mice pulsed with BrdU for 24 hr, immunostained for BrdU (green) or doublecortin (DCX, red), and counterstained with Hoechst (blue).

(E and F) Total cells positive for BrdU (E) and doublecortin (F) in the upper and lower DG blades, obtained by counting serial sections as in (D). *$p < 0.05$, $n = 3$ each.

(G) RT-PCR for *TAp73*, *ΔNp73*, and *p53* mRNAs in P3 *TAp73*$^{+/+}$ and *TAp73*$^{-/-}$ hippocampal neurospheres.

(H) P3 *TAp73*$^{+/+}$ and *TAp73*$^{-/-}$ hippocampal neurospheres immunostained for TAp73 (red) and counterstained with Hoechst 33258 (blue).

(I) Number of primary clonal neurospheres generated from 10,000 dissociated cells from P3 *TAp73*$^{+/+}$ and *TAp73*$^{-/-}$ hippocampi.

(J and K) Number (J) and mean diameter (K) of clonal neurospheres generated from 4,000 *TAp73*$^{+/+}$ and *TAp73*$^{-/-}$ P3 hippocampal neurosphere cells at one (2°/1°), two (3°/2°), and three (4°/3°) passages. *$p < 0.05$, $n = 3$ independent cultures.

(L) Immunostaining of *TA73*$^{+/+}$ and *TAp73*$^{-/-}$ hippocampal neurospheres for the proliferation marker Ki67 (red; cells were counterstained with Hoechst 33258, blue).

(M) Quantification of cultures similar to (L) for percentage of Ki67-positive cells. $p > 0.05$, $n = 3$. Error bars = S.E.M. See also Figure S1.

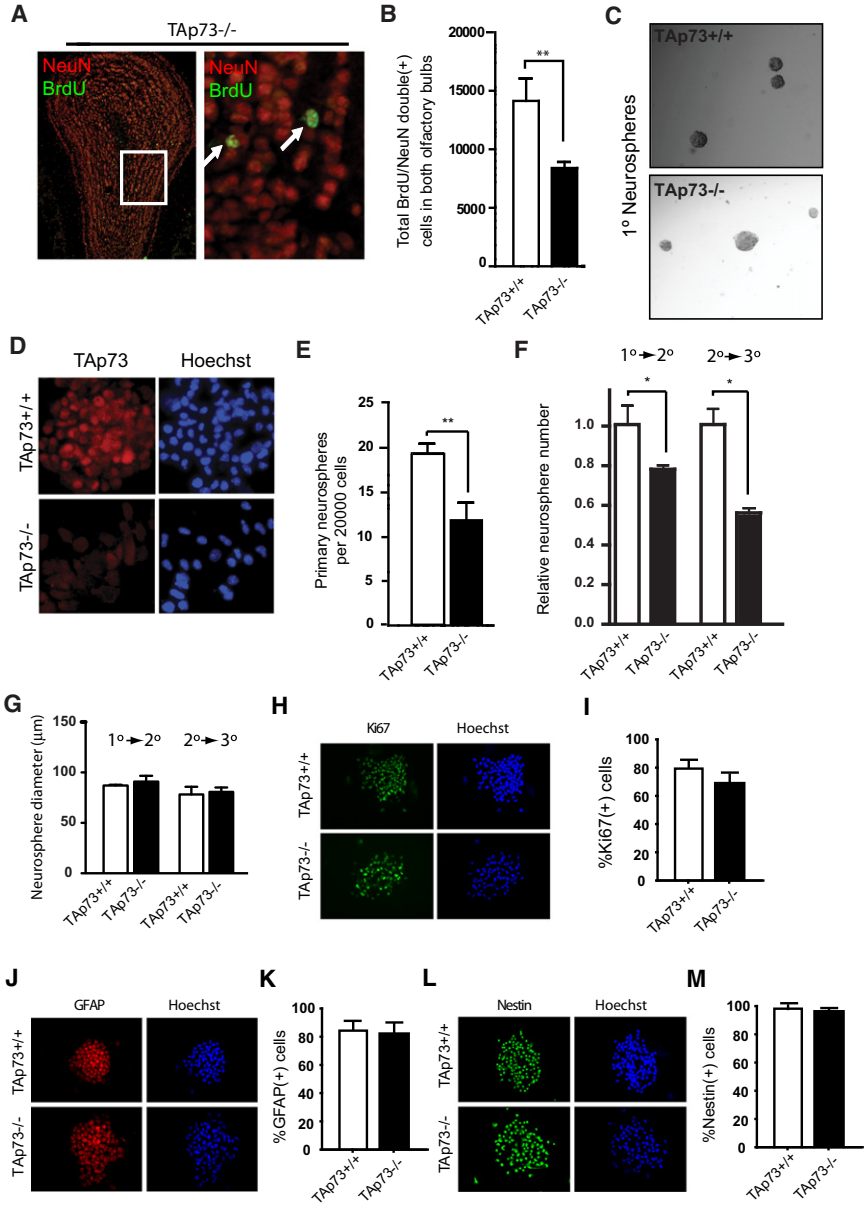

Figure 2. TAp73 Is Necessary for Maintenance of SVZ Precursors and Normal Olfactory Neurogenesis

(A) *Tap73*$^{-/-}$ olfactory bulb 1 month after BrdU injections, immunostained for BrdU (green) and NeuN (red) to detect newly born olfactory bulb neurons. The boxed area is shown at higher magnification at right. Arrows denote double-labeled cells.

(B) Total newly born neurons in *TAp73*$^{+/+}$ versus *TAp73*$^{-/-}$ olfactory bulbs as determined from serial sections similar to that in (A). **p < 0.01, n = 3 each.

(C and D) Adult SVZ *TAp73*$^{+/+}$ and *TAp73*$^{-/-}$ neurospheres shown (C) under phase illumination or (D) immunostained for TAp73 (red) and counterstained with Hoechst (blue).

(E) Clonal neurospheres generated from 20,000 primary SVZ cells from 2-month-old *TAp73*$^{+/+}$ versus *TAp73*$^{-/-}$ mice as shown in (C). **p < 0.01, n = 3.

(F and G) Number (F) and mean diameter (G) of clonal neurospheres generated from 4,000 *TAp73*$^{+/+}$ and *TAp73*$^{-/-}$ 2-month-old SVZ neurosphere cells at one (1°→2°), and two (2°→3°) passages. The data in (F) are expressed relative to the number of control *TAp73*$^{+/+}$ neurospheres. *p < 0.05, n = 3.

(H–M) Primary *TAp73*$^{+/+}$ and *TAp73*$^{-/-}$ SVZ neurospheres were immunostained for Ki67 (H, green), GFAP (J, red), or nestin (L, green) (cells were counterstained with Hoechst in blue) and the percentage of positive cells quantified (I, K, and M). In all cases, n = 3 independent neurosphere isolates, p > 0.05. Error bars = S.E.M. See also Figure S2.

from the lateral ventricle SVZ, where the relevant precursors reside [22] (Figure 2C). Immunostaining showed that most wild-type SVZ neurosphere cells expressed nuclear TAp73 (Figure 2D). However, relative to wild-type neurosphere numbers, the *TAp73*$^{-/-}$ SVZ cells generated only 61% as many neurospheres at 2 months of age (Figure 2E) and 55% as many at 1 year of age (19.4 ± 0.9 versus 10.7 ± 0.9 neurospheres per 20,000 SVZ cells, wild-type versus knockout; p < 0.05), indicating there were fewer SVZ stem cells. Moreover, when sequentially passaged, the *TAp73*$^{-/-}$ neurosphere-forming cells were progressively depleted (Figure 2F and Figure S2B). However, as for DG neurospheres, sphere diameter and percentage of Ki67-positive proliferating cells were similar between genotypes (Figures 2G–2I) as were the percentages of GFAP- and nestin-positive cells (Figures 2J–2M). Moreover, in both *TAp73*$^{+/+}$ and *TAp73*$^{-/-}$ neurospheres, only a few cleaved caspase-3-positive apoptotic cells were observed, and βIII-tubulin-positive neurons were undetectable (data not shown). Thus, TAp73 is specifically required for self-renewal and long-term maintenance of adult neural stem cells.

Hey2 Is Reduced in *Tap73*$^{-/-}$ Neural Precursors and Is a Transcriptional Target of TAp73

To ask how TAp73 regulates neural precursor maintenance, we turned to a more experimentally amenable system, developing cortical radial precursors [23–27], which ultimately contribute to the adult SVZ stem cell pool [28]. RT-PCR (Figure 3A) and immunostaining (Figure 3B) showed that TAp73 was expressed in the nuclei of nestin-positive precursors of the embryonic cortical ventricular zone (Figure 3B). As predicted by this finding, cultured E12 cortical precursors expressed *TAp73* mRNA and nuclear-localized TAp73 protein (Figures 3A and 3C). We then used acute genetic knockdown to ask whether TAp73 regulates maintenance of these precursors. We generated two shRNAs that target *TAp73* but not *ΔNp73* and assessed their efficacy by co-transfecting them into HEK293 cells with *TAp73* or, as controls, *ΔNp73*, *p53*, *TAp63*, or *ΔNp63*. We also used a control shRNA or two previously described shRNAs specific for *ΔNp73* [5]. Western blots showed that the *TAp73*-specific shRNAs decreased levels of TAp73, but not of ΔNp73, p53, TAp63, or ΔNp63 (Figure 3D). We then characterized cortical precursors that were cotransfected with these *TAp73* shRNAs

and EGFP. *TAp73* knockdown had no effect on apoptotic, cleaved caspase-3-positive cells (scrambled shRNA, 16.9% ± 2.0%; TAp73 shRNA TA-1, 15.3% ± 2.0%; TA-2, 19.3% ± 1.9%; $p > 0.05$, $n = 3$), but it did decrease the percentage of proliferating Ki67-positive precursors (Figure 3E). This decrease was rescued by cotransfection with human *TAp73* that is not targeted by the shRNA (Figure 3F).

To ask whether this proliferative effect was indicative of decreased maintenance, we transfected E13.5 radial precursors in vivo with *TAp73* or *ΔNp73* shRNAs by performing in utero electroporation (Figure 3G and Figures S3A and S3B). Analysis 2 days after electroporation showed that *TAp73* knockdown, but not *ΔNp73* knockdown ($p > 0.05$, $n = 3$), decreased the percentage of transfected cells expressing Ki67 (Figure 3H) or the radial precursor marker pax6 (Figure 3I). Thus, TAp73 is necessary to maintain the pool of cortical radial precursors.

We then used this system to determine how TAp73 promotes precursor maintenance. We initially examined the embryonic *TAp73*$^{-/-}$ cortex for genes that are known p53 family targets and/or that are implicated in neural precursor regulation. RT-PCR showed unaltered mRNA levels for *ΔNp73*, *p53*, and *TAp63*, the cell-cycle regulators *p16*, *p19*, *p21*, *p27*, *p57*, and the self-renewal gene *Bmi1* (Figure S3C). However, the mRNA for *Hey2*, a bHLH that promotes neural precursor maintenance when overexpressed [29], was decreased. In contrast, *Hey1* mRNA was unaffected. Quantitative real-time PCR confirmed these findings (Figure 3J) and showed a similar decrease in *Hey2* mRNA in neonatal *TAp73*$^{-/-}$ hippocampal neurospheres (Figure 3K). Analysis of the *Hey2* promoter defined a putative p53/p63/p73 consensus binding site 646 nucleotides upstream of the transcription start site (Figure 3L), suggesting that *Hey2* is a direct transcriptional target of TAp73. To test this idea, we performed chromatin immunoprecipitation (ChIP) assays on the P0 brain; in the *TAp73*$^{+/+}$ but not *TAp73*$^{-/-}$ cortex (Figure 3M) and hippocampus (data not shown), TAp73 was bound to a *Hey2* promoter region from −727 to −547, which brackets the p73 consensus site. To ask whether this binding promoted *Hey2* transcription, we cotransfected HEK293 cells for 2 days with a plasmid that included 3.5 kb of the *Hey2* promoter fused to the firefly *luciferase* gene [30] with or without a *TAp73* expression construct. TAp73 caused a 5-fold increase in firefly luciferase levels (Figure 3N) in this assay. Thus, TAp73 binds to and transactivates the *Hey2* promoter.

Hey2 Functions Downstream of FGF2 and TAp73 to Maintain Neural Precursors

These data suggest TAp73 promotes precursor maintenance by enhancing Hey2 transcription. However, although Hey2 is expressed in cortical precursors [29], its endogenous function is unknown. To ask whether Hey2 maintains precursors, we generated *Hey2* shRNAs, testing their efficacy by cotransfecting them with *Hey2* or *Hey1* constructs in HEK293 cells. Western blots (Figure 4A) showed that these shRNAs decreased Hey2 but not Hey1 levels. We then transfected these shRNAs into cortical precursors and analyzed them 2 to 3 days later. *Hey2* knockdown reduced proliferating Ki67-positive precursors (Figure 4B) and increased βIII-tubulin-positive newly born neurons (Figure 4C). We performed similar experiments in vivo, electroporating E13.5 cortices. *Hey2* knockdown decreased Ki67-positive precursors (Figures 4D and 4E) and increased newly born, doublecortin-positive neurons (Figure 4F). Thus, Hey2, like TAp73, maintains radial precursors in an undifferentiated state.

To ask whether TAp73 acts upstream of Hey2, we performed two final experiments. First, we asked whether FGF2, which is necessary for neural precursor maintenance [31], enhanced TAp73-mediated *Hey2* transcription. Precursors were established in FGF2 and then cultured with or without FGF2 for 3 days. Quantitative real-time PCR showed that *Hey2* but not *TAp73* mRNA levels increased approximately 2-fold in FGF2 (Figure 4G). ChIP assays showed that FGF2 also increased binding of TAp73 to the *Hey2* promoter TAp73 site (Figure 4H), potentially explaining the increase in *Hey2* mRNA. Second, we asked whether Hey2 reexpression could rescue the TAp73 knockdown phenotype. Precursors were cotransfected with scrambled or *TAp73* shRNAs with or without *Hey2* for 2 days. Hey2 transfection rescued the numbers of Ki67-positive proliferating precursors (Figure 4I). Thus, TAp73 acts upstream of Hey2 in a pathway that promotes the maintenance of neural precursor pools.

Discussion

Data presented here define a TAp73-Hey2 transcriptional pathway that, when disrupted, causes depletion of adult neural stem cells and decreases adult neurogenesis. Previous studies of p73 in the nervous system have largely focused upon ΔNp73, a potent neuronal survival protein [11–16]. However, a recent report showed that the hippocampal DG was aberrant in adult *TAp73*$^{-/-}$ mice [17], although the reasons for this phenotype were unknown. We show that this phenotype and the impaired adult neurogenesis we document here are due to loss of TAp73-mediated *Hey2* transcription. Hey2 is a negative bHLH that functions to suppress activator bHLHs [32, 33] and that acts downstream of Notch in cardiac cells and FGF12 in inner ear pillar cells [34]. Here, we found that Hey2 acts downstream of TAp73 and that FGF2, a key proliferation and maintenance factor for neural precursors [31], enhances TAp73-mediated transcription of *Hey2*. Thus, TAp73 and Hey2 join a small group of proteins that promote neural precursor maintenance and self-renewal, including Lfc [27], Bmi-1 [35], TLX [36], and the Notch pathway [37].

These findings have important implications for nervous system aging and neurodegeneration. Mice heterozygous for *p73* display age-dependent neurodegeneration [17], a phenotype attributed to loss of the ΔNp73 prosurvival isoform. However, our findings suggest that if adult neural stem cells play a role in maintaining the degenerating nervous system, then this premature aging phenotype may also be partially due to decreased TAp73 levels. Whether or not TAp73 plays a role in maintaining the brain and preventing premature cognitive aging is therefore a key question for future studies.

Experimental Procedures

Animals

This study was approved by The Hospital for Sick Children's Animal Care Committee and use was in accordance with Canadian Council on Animal Care guidelines. *TAp73*$^{+/-}$ mice were maintained on a C57BL/6 background as described [17].

Plasmids and Primers

The shRNAs against *TAp73* and *Hey2* were designed by OligoEngine software and cloned into the pSUPER retro.neo+gfp vector. The sequences were *TAp73* shRNA-1-, 5′-AGAGCCAGACAGCACCTAC-3′, *TAp73* shRNA-2,

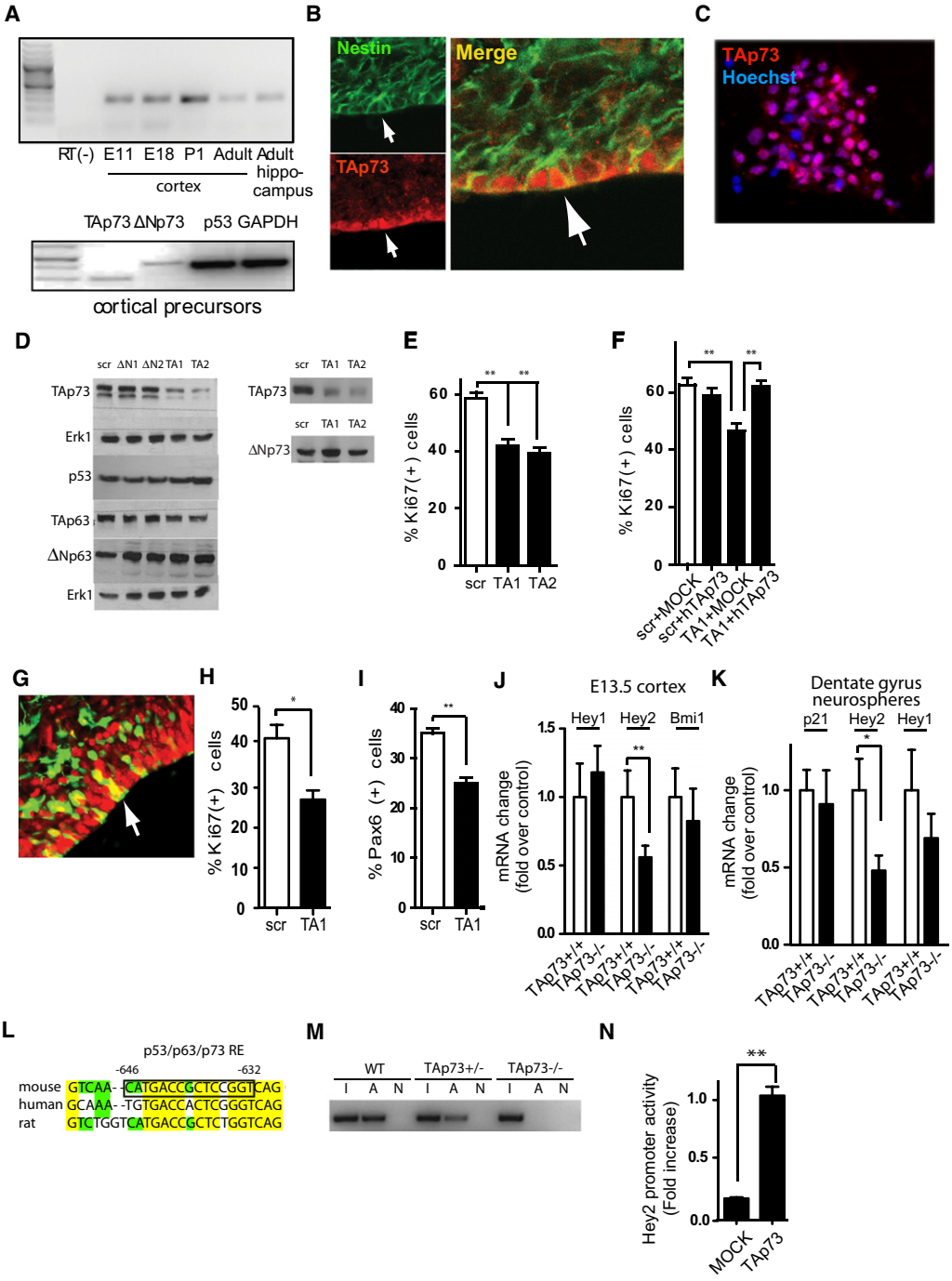

Figure 3. Expression of Hey2, a Direct Transcriptional Target of TAp73, Is Decreased in *Tap73*$^{-/-}$ Precursors

(A) RT-PCR for *TAp73* in the developing cortex (top), and cortical precursors cultured 1 day (bottom).

(B) Immunostaining for nestin (green) and TAp73 (red) in the E13 cortical neuroepithelium adjacent to the ventricle. Arrows denote double-labeled cells.

(C) Cortical precursors cultured 1 day, immunostained for TAp73 (red) and counterstained with Hoechst (blue).

(D) Western blots of HEK293 cells cotransfected with shRNAs targeted to *ΔNp73* (ΔN1, ΔN2) or to *TAp73* (TA1, TA2) together with plasmids encoding *TAp73*, *ΔNp73*, *p53*, *ΔNp63*, or *TAp63* and probed with antibodies to the indicated proteins. Blots were reprobed with anti-Erk1 to ensure equal loading.

(E) Percentage of Ki67-positive precursors (E) in cortical cultures cotransfected with EGFP and scrambled (scr) or *TAp73* shRNAs (TA1 and TA2) for 2 days. **$p < 0.01$, $n = 3$.

(F) Rescue experiment quantifying Ki67-positive proliferating precursors in cortical cultures cotransfected with EGFP and scrambled (scr) or *TAp73* shRNA with or without a human *TAp73* cDNA (hTAp73) for 2 days. Some cells received empty vector in place of human *TAp73* cDNA (MOCK). **$p < 0.01$, $n = 3$.

(G) Cortical section electroporated with EGFP and *TAp73* shRNA at E13.5 and immunostained for EGFP (green) and Ki67 (red) at E15/E16. Arrow denotes a double-labeled cell.

(H and I) Quantification of cortical sections similar to (G), electroporated with scrambled (scr) or *TAp73* shRNA for the percentage of transfected, Ki67-positive cells (H) or pax6-positive precursors (I). *$p < 0.05$, $n = 3$.

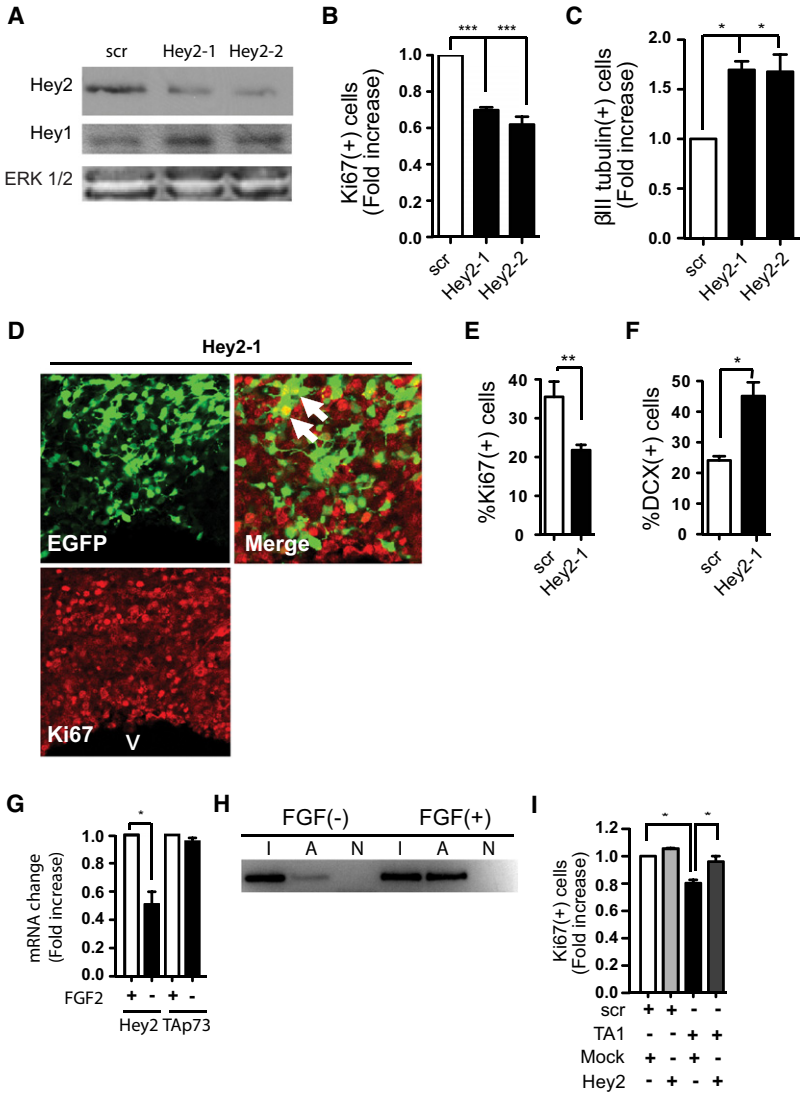

Figure 4. Hey2 Promotes Maintenance of Neural Precursors and Is Downstream of TAp73

(A)Western blots of HEK293 cells cotransfected with *Hey2* or *Hey1* expression plasmids and *Hey2* shRNAs (Hey2-1, Hey2-2) and probed with antibodies to Hey2, Hey1, or Erk1/2 to assure equal protein loading.

(B and C) Relative numbers of Ki67-positive precursors (B) or βIII-tubulin-positive neurons (C) in cortical cultures cotransfected with EGFP and scrambled shRNA or shRNAs to *Hey2*. *p < 0.05, ***p < 0.005, n = 3.

(D) Cortical section electroporated with EGFP and *Hey2* shRNA at E13.5 and immunostained 2 days later for EGFP (green) and (Ki67) (red). Arrows denote double-labeled cells. V = ventricle.

(E and F) Quantification of cortices electroporated with *Hey2* shRNA or scrambled shRNA as in (D) for transfected, Ki67-positive precursors (E) or doublecortin-positive neurons (F). *p < 0.05, **p < 0.01, n = 3.

(G) Quantitative real-time PCR for *Hey2* and *TAp73* mRNAs in precursors cultured 3 days with or without FGF2. *p < 0.01, n = 3.

(H) ChIP assays for TAp73 binding to the *Hey2* promoter region containing the p53 family consensus site in cortical precursors cultured 3 days with or without FGF2. Shown is a representative gel loaded with the amplified promoter regions from nonimmunoprecipitated input (I), extracts immunoprecipitated with anti-TAp73(A), or control nonimmune IgG (N).

(I) Rescue experiment quantifying the relative number of Ki67-positive proliferating precursors that were cotransfected with EGFP and scrambled or *TAp73* shRNA with or without a *Hey2* cDNA expression plasmid for 2 days. Some cells received the empty vector rather than *Hey2* cDNA (Mock). *p < 0.05, n = 3. Error bars = S.E.M.

5′-GAGCCAGACAGCACCTACT-3′, *Hey2* shRNA-1, 5′-GGTCCAATTCACC GACAAC-3′, and *Hey2* shRNA-2, 5′-CCAATTCACCGACAACTAC-3′. The human *ΔNp73α* and *TAp73α* expression plasmids were previously published [13]; the mouse *Hey2* expression vector in pcDNA3.1 and the mouse *Hey2* promoter containing pGL2 basic vector were kind gifts from Drs. Ryoichiro Kageyama [29] and Larry Kedes [30], respectively. All primer information is in Supplemental Information.

Precursor Cultures

The E12-E13 cortical precursors from CD1 mice were cultured in 40 ng/mL FGF2 as described [5, 23–27] at a density of 125,000 ~ 150,000 cells/well in four-well chamber slides. For transfections, 1 hr after plating, 1 μg total DNA and 1.5 μl Fugene 6.0 (Roche) mixed with 100 μl of Opti-MEM (Invitrogen) were incubated at room temperature for 45 min and added to the cultures. For adult SVZ neurospheres, the subependyma of the lateral ventricle was dissected and dissociated as described [38]. Cell density and viability were determined with trypan blue. Cells were cultured in the neurosphere assay under clonal conditions [22] at 10 cells/μL in six-well (2 mL/well) ultralow attachment dishes (Corning) in serum-free medium containing 20 ng/mL EGF (Sigma), 10 ng/mL FGF2 (Sigma), and 2 μg/mL heparin (Sigma). Sphere number was counted after 6 days; only colonies of at least 10 cells were counted as spheres. For postnatal hippocampal neurospheres, the third most dorsal aspect of the hippocampus was dissected and tissue was trimmed to remove the walls of the third and lateral ventricles [21]. Tissue was mechanically dissociated, and spheres were cultured and counted as for SVZ neurospheres. For the assay of self-renewal, neurospheres were mechanically dissociated into single cell, passed through a cell strainer, cultured as for primary cultures and spheres counted after 4 days.

Immunocytochemistry

Immunocytochemical analysis of cultured cells was performed as described [23–27]. Neurospheres were plated for immunocytochemistry by cytospins

(J and K) Quantitative real-time PCR for *Hey1*, *Hey2*, *Bmi1*, and *p21* mRNAs in *TAp73*$^{+/+}$ and *TAp73*$^{-/-}$ E13.5 cortex (J) or P0-P3 hippocampal neurospheres (K). *p < 0.05, **p < 0.01, n = 3.

(L) Consensus *p53* family response element in the proximal *Hey2* rat, mouse and human promoter region. Yellow highlights nucleotide identity between all 3, and green identity in 2 of 3 species.

(M) ChIP assays where chromatin from *TAp73*$^{+/+}$, *TAp73*$^{+/-}$ and *TAp73*$^{-/-}$ P0 cortices was immunoprecipitated with anti-TAp73 and PCR was used to amplify a promoter region encompassing the p53 family binding site. Gel was loaded with PCR product from nonimmunoprecipitated input (I), anti-TAp73 precipitate (A), or control nonimmune IgG precipitate (N). Results are representative of three independent experiments.

(N) Heterologous transcriptional assays where HEK293 cells were cotransfected with *TAp73* and a plasmid encoding a 3.5 kb *Hey2* promoter fragment containing the p53 family consensus site driving expression of firefly *luciferase*. Firefly luciferase activity was normalized to Renilla luciferase levels driven from a control plasmid cotransfected into the same cells. *p < 0.01, n = 3. Error bars = S.E.M. See also Figure S3.

(Thermo Shandon). All antibody information is in Supplemental Experimental Procedures. For quantification, approximately 200 cells from 8–10 randomly chosen fields (per condition per experiment) were counted. Images were acquired with Northern Eclipse software (Empix, Mississauga, Ontario, Canada) with a Sony (Tokyo, Japan) XC-75CE CCD video camera.

In Utero Electroporations and Analyses

In utero electroporations were performed on embryonic day 13–14 with a square electroporator CUY21 EDIT (TR Tech, Japan) delivering five 50 ms pulses of 50 V with 950 ms intervals per embryo, as described [23–27]. Embryos were injected with a total of 4.0 ug DNA per embryo, mixing the EGFP expression plasmid at a 1:3 ratio with the shRNA constructs; 0.05% trypan blue was coinjected as a tracer. In utero electroporated brains were drop fixed in 4% paraformaldehyde, cryosectioned at 16–20 um, and immunocytochemistry was performed as described [23–27]. Sections with a similar anatomical distribution of EGFP expression were chosen for analysis, as described [5, 27]. A total of three to four sections were analyzed per animal on a Zeiss Pascal confocal microscope (Oberkochen, Germany) by taking up to three 8–10 μm z-stack pictures per section with a 40× objective as described [5, 27]. Statistics were performed with either the Student's t test or one-way ANOVA, as appropriate.

Neuroanatomy and BrdU Labeling

Nissl staining and immunohistochemistry of neonatal and adult brains, with the exception of the BrdU experiments, were performed as described [13]. For hippocampal BrdU experiments, 100 mg/kg BrdU (Sigma) was administered intraperitoneally; mice were sacrificed by sodium pentobarbital overdose and transcardially perfused with PBS followed by 4% PFA. Brains were postfixed overnight and the hippocampus was sectioned transversally on a vibratome at 40 μm. Every fourth hippocampal section was analyzed immunocytochemically for BrdU as described [39]. All BrdU-labeled nuclei in the SGZ (defined as two cell diameters beneath the granule cell layer), were counted, and blade length was measured. For SVZ experiments, mice were injected with 60 mg/kg BrdU intraperitoneally every 3 hr for five injections and sacrificed 30 d later [40]. Animals were overdosed with pentobarbital and perfused transcardially with PBS and 4% paraformaldehyde. Brains were postfixed, cryoprotected, and cryosectioned at 14 μm. Sections were incubated in 1 N HCl at 60°C for 30 min, rinsed in PBS, incubated in rat anti-BrdU antibody at 4°C overnight and then in Alexa 488 donkey anti-rat antibody for 2 hr, followed by sequential immunostaining with anti-NeuN, followed by an Alexa Fluor 555-conjugated goat anti-mouse secondary antibody. The main olfactory bulb was serially sectioned, and the total number of BrdU-labeled cells determined in the granule cell layer of every tenth section, extending just anterior to the rostral portion of the accessory olfactory bulb.

Western Blotting

Western blots were performed with 20–30 μg of HEK293 protein lysates 2 days after transfections, as described [5, 41]. Antibodies are listed in Supplemental Experimental Procedures.

RT-PCR Analysis

RNA was isolated by the Trizol method (Invitrogen). RNA was treated with DNase (Fermentas) to avoid contamination with genomic DNA. Reverse transcription was carried out with RevertAid H Minus M-MuLV Reverse Transcriptase (Fermentas) primed with random hexamers, according to manufacturer's instructions. Primer information is in Supplemental Information. For quantitative real-time PCR, total RNA was extracted with Trizol reagent (Invitrogen) and the RNeasy kit (QIAGEN). cDNA for qRT-PCR was prepared with SuperScript III First-Strand Synthesis SuperMix (Invitrogen). Real-time PCR was performed according to the manufacturer's specifications with Chromo4 Real-Time PCR Detection System (Bio-Rad) and a Platinum Quantitative PCR Super-Mix-UDG (Invitrogen). Samples were analyzed in triplicate and were normalized to *β-actin* for each reaction. All PCR products were single bands with predicted molecular weights.

Chromatin Immunoprecipitation Assays

Chromatin immunoprecipitation(ChIP) assays of cortical tissue were performed as described [42]. Chromatin was immunoprecipitated with an affinity purified rabbit polyclonal antibody to TAp73 (Bethyl Laboratories) or rabbit nonimmune IgG antibody. One-tenth of the lysate was kept to quantify the amount of DNA present in different samples before immunoprecipitation (input). PCR amplification was performed with primers that amplify the genomic fragment from −727 bp to −547 bp of the mouse *Hey2* promoter region (GenBank accession number AY059384, –3521bp): 5′-TGACCACAACCTAGAGGCT-3′ and 5′-GTGAGCGTGTGTGACGT-3′. Varying amounts of template were used to ensure that results were within the linear range of the PCR reaction.

Heterologous Transcriptional Assays

Human embryonic kidney (HEK) 293 cells (6×10^4 per well of a six-well culture plate) were transiently cotransfected with a total amount of 1.5 μg of plasmid DNA: 1.0 μg *Hey2* promoter-pGL2 firefly luciferase reporter vector [30], 100 ng of the pRL-TK Renilla *luciferase* control vector (Promega), and/or 0.5 μg of the indicated pCDNA3.1 mouse *TAp73α* expression plasmid or empty control vector, using Lipofectamine 2000 Transfection Reagent (Invitrogen) according to the manufacturer's protocol. Seventy-two hours after transfection, the cells were washed (1 × PBS) and then lysed (300 μl passive lysis buffer, Promega) with gentle rocking (21°C, 15 min). Activities of luciferases encoded by experimental and internal control plasmids were measured sequentially with the Dual Luciferase Assay kit (Promega) and a Lumat LB 9507 Single Tube Luminometer (Berthold Technologies) according to the manufacturer's protocol. Transfections were repeated a minimum of three times with different cultures of HEK293 cells.

Accession Numbers

The GenBank accession number for the *Hey2* promoter region sequence reported in this paper is AY059384.

Supplemental Information

Supplemental Information includes Supplemental Experimental Procedures and three figures and can be found with this article online at doi:10.1016/j.cub.2010.10.029.

Acknowledgments

This work was supported by Canadian Institutes of Health Research (CIHR) Grants MOP13958 and FRN38021 to F.D.M. and D.R.K. F.D.M. and D.R.K. are Canada Research Chairs, and F.D.M. is a Howard Hughes Medical Institute International Research Scholar. M.F. was supported by fellowships from the Japan Society for the Promotion of Science (JSPS), Kanae Foundation, the Japan Heart Foundation, and the SickKids Foundation, and I.C.G.W. by a CIHR fellowship, while C.B.D. and A.P. were supported by studentships from National Sciences and Engineering Council of Canada and CIHR and the Hospital for Sick Children Foundation, respectively. We thank Nadia Sachewsky, Cindi Morshead, Derek van der Kooy, Satoshi Inoue, and Meredith Irwin for their help and input; Benigno Aquino for technical assistance; and Kaplan/Miller laboratory members for advice and assistance.

Received: July 14, 2010
Revised: September 16, 2010
Accepted: October 12, 2010
Published online: November 11, 2010

References

1. Sharpless, N.E., and DePinho, R.A. (2007). How stem cells age and why this makes us grow old. Nat. Rev. Mol. Cell Biol. *8*, 703–713.
2. Lavigueur, A., Maltby, V., Mock, D., Rossant, J., Pawson, T., and Bernstein, A. (1989). High incidence of lung, bone, and lymphoid tumors in transgenic mice overexpressing mutant alleles of the p53 oncogene. Mol. Cell. Biol. *9*, 3982–3991.
3. Tyner, S.D., Venkatachalam, S., Choi, J., Jones, S., Ghebranious, N., Igelmann, H., Lu, X., Soron, G., Cooper, B., Brayton, C., et al. (2002). p53 mutant mice that display early ageing-associated phenotypes. Nature *415*, 45–53.
4. Keyes, W.M., Wu, Y., Vogel, H., Guo, X., Lowe, S.W., and Mills, A.A. (2005). p63 deficiency activates a program of cellular senescence and leads to accelerated aging. Genes Dev. *19*, 1986–1999.
5. Dugani, C.B., Paquin, A., Fujitani, M., Kaplan, D.R., and Miller, F.D. (2009). p63 antagonizes p53 to promote the survival of embryonic neural precursor cells. J. Neurosci. *29*, 6710–6721.
6. Meletis, K., Wirta, V., Hede, S.M., Nistér, M., Lundeberg, J., and Frisén, J. (2006). p53 suppresses the self-renewal of adult neural stem cells. Development *133*, 363–369.

7. Senoo, M., Pinto, F., Crum, C.P., and McKeon, F. (2007). p63 Is essential for the proliferative potential of stem cells in stratified epithelia. Cell *129*, 523–536.
8. Suh, E.K., Yang, A., Kettenbach, A., Bamberger, C., Michaelis, A.H., Zhu, Z., Elvin, J.A., Bronson, R.T., Crum, C.P., and McKeon, F. (2006). p63 protects the female germ line during meiotic arrest. Nature *444*, 624–628.
9. Su, X., Paris, M., Gi, Y.J., Tsai, K.Y., Cho, M.S., Lin, Y.L., Biernaskie, J.A., Sinha, S., Prives, C., Pevny, L.H., et al. (2009). TAp63 prevents premature aging by promoting adult stem cell maintenance. Cell Stem Cell *5*, 64–75.
10. Wetzel, M.K., Naska, S., Laliberté, C.L., Rymar, V.V., Fujitani, M., Biernaskie, J.A., Cole, C.J., Lerch, J.P., Spring, S., Wang, S.H., et al. (2008). p73 regulates neurodegeneration and phospho-tau accumulation during aging and Alzheimer's disease. Neuron *59*, 708–721.
11. Yang, A., Walker, N., Bronson, R., Kaghad, M., Oosterwegel, M., Bonnin, J., Vagner, C., Bonnet, H., Dikkes, P., Sharpe, A., et al. (2000). p73-deficient mice have neurological, pheromonal and inflammatory defects but lack spontaneous tumours. Nature *404*, 99–103.
12. Pozniak, C.D., Radinovic, S., Yang, A., McKeon, F., Kaplan, D.R., and Miller, F.D. (2000). An anti-apoptotic role for the p53 family member, p73, during developmental neuron death. Science *289*, 304–306.
13. Pozniak, C.D., Barnabé-Heider, F., Rymar, V.V., Lee, A.F., Sadikot, A.F., and Miller, F.D. (2002). p73 is required for survival and maintenance of CNS neurons. J. Neurosci. *22*, 9800–9809.
14. Tissira, F., Ravnia, A., Achouria, Y., Riethmacherb, D., Meyerc, G., and Goffineta, A. (2009). DeltaNp73 regulates neuronal survival in vivo. Proc. Natl. Acad. Sci. USA *106*, 16871–16876.
15. Wilhelm, M.T., Rufini, A., Wetzel, M.K., Tsuchihara, K., Inoue, S., Tomasini, R., Itie-Youten, A., Wakeham, A., Arsenian-Henriksson, M., Melino, G., et al. (2010). Isoform-specific p73 knockout mice reveal a novel role for delta Np73 in the DNA damage response pathway. Genes Dev. *24*, 549–560.
16. Walsh, G.S., Orike, N., Kaplan, D.R., and Miller, F.D. (2004). The invulnerability of adult neurons: a critical role for p73. J. Neurosci. *24*, 9638–9647.
17. Tomasini, R., Tsuchihara, K., Wilhelm, M., Fujitani, M., Rufini, A., Cheung, C.C., Khan, F., Itie-Youten, A., Wakeham, A., Tsao, M.S., et al. (2008). TAp73 knockout shows genomic instability with infertility and tumor suppressor functions. Genes Dev. *22*, 2677–2691.
18. Roybon, L., Hjalt, T., Stott, S., Guillemot, F., Li, J.Y., and Brundin, P. (2009). Neurogenin2 directs granule neuroblast production and amplification while NeuroD1 specifies neuronal fate during hippocampal neurogenesis. PLoS ONE *4*, e4779.
19. Altman, J., and Bayer, S.A. (1990). Mosaic organization of the hippocampal neuroepithelium and the multiple germinal sources of dentate granule cells. J. Comp. Neurol. *301*, 325–342.
20. Zhao, C., Deng, W., and Gage, F.H. (2008). Mechanisms and functional implications of adult neurogenesis. Cell *132*, 645–660.
21. Seaberg, R.M., and van der Kooy, D. (2002). Adult rodent neurogenic regions: the ventricular subependyma contains neural stem cells, but the dentate gyrus contains restricted progenitors. J. Neurosci. *22*, 1784–1793.
22. Coles-Takabe, B.L., Brain, I., Purpura, K.A., Karpowicz, P., Zandstra, P.W., Morshead, C.M., and van der Kooy, D. (2008). Don't look: growing clonal versus nonclonal neural stem cell colonies. Stem Cells *26*, 2938–2944.
23. Barnabé-Heider, F., Wasylnka, J.A., Fernandes, K.J.L., Porsche, C., Sendtner, M., Kaplan, D.R., and Miller, F.D. (2005). Evidence that embryonic neurons regulate the onset of cortical gliogenesis via cardiotrophin-1. Neuron *48*, 253–265.
24. Gauthier, A.S., Furstoss, O., Araki, T., Chan, R., Neel, B.G., Kaplan, D.R., and Miller, F.D. (2007). Control of CNS cell-fate decisions by SHP-2 and its dysregulation in Noonan syndrome. Neuron *54*, 245–262.
25. Paquin, A., Barnabé-Heider, F., Kageyama, R., and Miller, F.D. (2005). CCAAT/enhancer-binding protein phosphorylation biases cortical precursors to generate neurons rather than astrocytes in vivo. J. Neurosci. *25*, 10747–10758.
26. Bartkowska, K., Paquin, A., Gauthier, A.S., Kaplan, D.R., and Miller, F.D. (2007). Trk signaling regulates neural precursor cell proliferation and differentiation during cortical development. Development *134*, 4369–4380.
27. Gauthier-Fisher, A., Lin, D.C., Greeve, M., Kaplan, D.R., Rottapel, R., and Miller, F.D. (2009). Lfc and Tctex-1 regulate the genesis of neurons from cortical precursor cells. Nat. Neurosci. *12*, 735–744.
28. Willaime-Morawek, S., Seaberg, R.M., Batista, C., Labbé, E., Attisano, L., Gorski, J.A., Jones, K.R., Kam, A., Morshead, C.M., and van der Kooy, D. (2006). Embryonic cortical neural stem cells migrate ventrally and persist as postnatal striatal stem cells. J. Cell Biol. *175*, 159–168.
29. Sakamoto, M., Hirata, H., Ohtsuka, T., Bessho, Y., and Kageyama, R. (2003). The basic helix-loop-helix genes Hesr1/Hey1 and Hesr2/Hey2 regulate maintenance of neural precursor cells in the brain. J. Biol. Chem. *278*, 44808–44815.
30. Iso, T., Sartorelli, V., Chung, G., Shichinohe, T., Kedes, L., and Hamamori, Y. (2001). HERP, a new primary target of Notch regulated by ligand binding. Mol. Cell. Biol. *21*, 6071–6079.
31. Raballo, R., Rhee, J., Lyn-Cook, R., Leckman, J.F., Schwartz, M.L., and Vaccarino, F.M. (2000). Basic fibroblast growth factor (Fgf2) is necessary for cell proliferation and neurogenesis in the developing cerebral cortex. J. Neurosci. *20*, 5012–5023.
32. Kageyama, R., Ohtsuka, T., Hatakeyama, J., and Ohsawa, R. (2005). Roles of bHLH genes in neural stem cell differentiation. Exp. Cell Res. *306*, 343–348.
33. Fischer, A., Schumacher, N., Maier, M., Sendtner, M., and Gessler, M. (2004). The Notch target genes Hey1 and Hey2 are required for embryonic vascular development. Genes Dev. *18*, 901–911.
34. Doetzlhofer, A., Basch, M.L., Ohyama, T., Gessler, M., Groves, A.K., and Segil, N. (2009). Hey2 regulation by FGF provides a Notch-independent mechanism for maintaining pillar cell fate in the organ of Corti. Dev. Cell *16*, 58–69.
35. Molofsky, A.V., Pardal, R., Iwashita, T., Park, I.K., Clarke, M.F., and Morrison, S.J. (2003). Bmi-1 dependence distinguishes neural stem cell self-renewal from progenitor proliferation. Nature *425*, 962–967.
36. Zhang, C.L., Zou, Y., He, W., Gage, F.H., and Evans, R.M. (2008). A role for adult TLX-positive neural stem cells in learning and behaviour. Nature *451*, 1004–1007.
37. Hitoshi, S., Alexson, T., Tropepe, V., Donoviel, D., Elia, A.J., Nye, J.S., Conlon, R.A., Mak, T.W., Bernstein, A., and van der Kooy, D. (2002). Notch pathway molecules are essential for the maintenance, but not the generation, of mammalian neural stem cells. Genes Dev. *16*, 846–858.
38. Kolb, B., Morshead, C., Gonzalez, C., Kim, M., Gregg, C., Shingo, T., and Weiss, S. (2007). Growth factor-stimulated generation of new cortical tissue and functional recovery after stroke damage to the motor cortex of rats. J. Cereb. Blood Flow Metab. *27*, 983–997.
39. Wojtowicz, J.M., and Kee, N. (2006). BrdU assay for neurogenesis in rodents. Nat. Protoc. *1*, 1399–1405.
40. Morshead, C.M., Craig, C.G., and van der Kooy, D. (1998). In vivo clonal analyses reveal the properties of endogenous neural stem cell proliferation in the adult mammalian forebrain. Development *125*, 2251–2261.
41. Jacobs, W.B., Govoni, G., Ho, D., Atwal, J.K., Barnabe-Heider, F., Keyes, W.M., Mills, A.A., Miller, F.D., and Kaplan, D.R. (2005). p63 is an essential proapoptotic protein during neural development. Neuron *48*, 743–756.
42. Wang, J., Weaver, I.C., Gauthier-Fisher, A., Wang, H., He, L., Yeomans, J., Wondisford, F., Kaplan, D.R., and Miller, F.D. (2010). CBP histone acetyltransferase activity regulates embryonic neural differentiation in the normal and Rubinstein-Taybi syndrome brain. Dev. Cell *18*, 114–125.